ASIAN JOURNAL OF PHARMACEUTICAL AND CLINICAL RESEARCH

INNOVARE ACADEMIC SCIENCES
Knowledge to Innovation

Vol 19, Issue 4, 2026

Online - 2455-3891
Print - 0974-2441

Research Article

CHLOROGENIC ACID FROM *SARGASSUM ILICIFOLIUM* ATTENUATES CHEMOTHERAPY-INDUCED NEPHROTOXICITY THROUGH SIRT1 ACTIVATION

CHANDUPATLA RAMYA[1]*, RAHUL INGLE[2], PATCHIGONDLA REENA SOWMYA[1], GURUSAMY MARIAPPAN[3]

[1]Department of Pharmacology, Datta Meghe College of Pharmacy, Datta Meghe Institute of Higher Education and Research (Deemed to be University), Wardha, Maharashtra, India. [2]Department of Pharma Chemistry, Datta Meghe College of Pharmacy, Datta Meghe Institute of Higher Education and Research (Deemed to be University), Wardha, Maharashtra, India. [3]Department of Pharm Chemistry, St Mary's College of Pharmacy, Secunderabad, Telangana, India.

***Corresponding author: Chandupatla Ramya; Email: padigela.ramya@gmail.com**

Received: 20 September 2025, Revised and Accepted: 23 February 2026

ABSTRACT

Objectives: The present study aimed to evaluate the nephroprotective potential of *Sargassum ilicifolium* extract against cyclophosphamide (CPM) drug-induced kidney injury using integrated *in vitro*, *in silico*, and *in vivo* approaches, with emphasis on sirtuin 1 (SIRT1)-mediated mechanisms.

Methods: The ethanolic extract of *S. ilicifolium* was characterized using ultraviolet-visible spectroscopy, Fourier transform infrared, nuclear magnetic resonance, and liquid chromatography-mass spectrometry (LC-MS) analyses. Cytotoxicity and SIRT1 expression were assessed by SIRT1 assay in HK-2 cells, supported by molecular docking studies of chlorogenic acid (CGA) with SIRT1. Acute oral toxicity and nephroprotective efficacy were evaluated in cyclophosphamide-induced renal injury in rats through biochemical and histopathological analyses.

Results: LC-MS analysis revealed diverse phytochemicals, with CGA identified as the major constituent (*m/z* 354.31, retention time 4.5 min). CGA exhibited low cytotoxicity (IC_{50}=237.6 µg/mL) and significantly restored SIRT1 expression in HK-2 cells. Docking studies showed favorable binding with SIRT1 (−5.85 kcal/mol). *In vivo*, cyclophosphamide markedly elevated serum creatinine (1.57±0.085 mg/dL), uric acid (5.95±0.267 mg/dL), and urea (98.23±3.549 mg/dL), whereas treatment with *S. ilicifolium* (400 mg/kg) normalized these biomarkers (~0.56 mg/dL creatinine, ~2.0 mg/dL uric acid, ~28–29 mg/dL urea) and preserved renal histoarchitecture. Cyclophosphamide induced electrolyte imbalance and renal tubular dysfunction in rats, whereas treatment with *S. ilicifolium* extract restored sodium (144.57±3.459 mmol/L) and chloride (101.22±0.465 mmol/L) levels and shifted potassium and calcium closer to the normal range, indicating renoprotective activity. All data were tested for statistical significance at **p<0.01 and ***p<0.001 versus the negative control.

Conclusion: *S. ilicifolium* extract exhibited significant nephroprotective activity through SIRT1 upregulation, biochemical normalization, and renal tissue preservation, supporting its potential as a natural therapeutic candidate for drug-induced kidney damage.

Keywords: *Sargassum ilicifolium*, Nephroprotection, Sirtuin 1, Chlorogenic acid.

 DOI: http://dx.doi.org/10.22159/ajpcr.2026v19i4.56942. Journal homepage: https://innovareacademics.in/journals/index.php/ajpcr

INTRODUCTION

Acute kidney injury (AKI) affects approximately 13.3 million individuals worldwide each year and is responsible for nearly 1.7 million deaths annually [1,2]. Survivors of AKI remain at a significantly increased risk of developing chronic kidney disease (CKD) and may progress to end-stage kidney disease, irrespective of complete renal recovery. Although AKI and CKD were previously regarded as distinct clinical entities, they are now recognized as a continuum of progressive kidney dysfunction [3]. Importantly, certain patients exhibit renal impairment that does not meet the established diagnostic criteria for either AKI or CKD, highlighting gaps in current clinical classifications [4].

Kidney disease is mediated by complex pathological mechanisms, including oxidative stress, inflammation, mitochondrial dysfunction, apoptosis, and fibrosis, which collectively contribute to progressive renal injury. Excessive generation of reactive oxygen species and activation of inflammatory pathways such as nuclear factor kappa B (NF-κB) play a central role in renal cellular damage and functional decline [5,6]. Sirtuin 1 (SIRT1), a NAD^+-dependent deacetylase, has emerged as a critical nephroprotective regulator by suppressing oxidative stress and inflammation, improving mitochondrial function, and inhibiting apoptosis and renal fibrosis through modulation of p53, FOXO transcription factors, NF-κB, and PGC-1α signaling pathways [7].

SIRT1 plays a critical protective role in acute kidney disease (AKI) by modulating cellular responses to renal stress and injury. Activation of SIRT1 reduces oxidative stress and inflammatory signaling, preserves mitochondrial function, and inhibits apoptosis in renal tubular epithelial cells through regulation of key molecular pathways involving p53, FOXO transcription factors, and NF-κB. Experimental evidence demonstrates that enhancement of SIRT1 activity significantly attenuates ischemic and drug-induced renal injury and limits progression toward CKD [8-10]. Currently, effective and targeted therapies for AKI are unavailable in the clinic, except for supportive management [11]. The Kidney Disease: Improving Global Outcomes guidelines for AKI recommend implementing various supportive measures in high-risk patients, including volume management, maintenance of adequate blood pressure, and judicious avoidance of nephrotoxins [12]. Therefore, effective therapeutic strategies are urgently needed based on the pathogenesis of AKI.

Brown seaweeds, particularly *Sargassum ilicifolium* [13], found in tropical and subtropical waters, have been traditionally used in various cultures for their medicinal properties. Chemical analyses have identified a diverse array of active compounds, including sulphated polysaccharides (fucoidans), polyphenols (phlorotannins), sterols (fucosterol), pigments (fucoxanthin), and minerals [14]. These compounds have exhibited anti-oxidant, anti-inflammatory, anti-obesity, anti-hypertensive, and anti-diabetic effects in laboratory

studies. Polysaccharides from *S. ilicifolium* are particularly effective in scavenging free radicals and inhibiting α-glucosidase, while phlorotannins and fucosterol demonstrate anti-inflammatory and cholesterol-lowering properties [15]. These bioactivities suggest that *S. ilicifolium* could serve as a complementary or supplementary therapy to mitigate diabetic complications, including nephropathy, potentially through pathways involving SIRT1. *S. ilicifolium* serves as a supportive or adjunct treatment for managing kidney complications, particularly nephropathy, by acting through mechanisms that may intersect with SIRT1-regulated pathways. This research explores combating AKI by activating SIRT1 and by utilizing the bioactive compounds of *S. ilicifolium*, with the aim of reducing renal cell damage to slow or reverse disease progression.

METHODS

All chemicals and solvents used in the study were of analytical grade and were purchased from Merck (India) Ltd. and used without further purification. Fourier transform infrared (FTIR) spectra were recorded using a PerkinElmer FTIR spectrophotometer (Model 1650) in the range of 4000–400 cm^{-1}. ^{1}H and ^{13}C NMR spectra were acquired on a Bruker Avance 400 MHz nuclear magnetic resonance (NMR) spectrometer using deuterated dimethyl sulfoxide (DMSO-d_6) as the solvent and tetramethylsilane (TMS) as the internal standard. Mass spectrometric analysis was carried out using an Agilent 5977C mass spectrometer under standard operating conditions.

Collection of *S. ilicifolium*

Fresh samples of the brown alga *S. ilicifolium* were collected from the intertidal zone near Rameswaram, Tamil Nadu, India (9.2876° N, 79.3173° E) during low tide. The algae were authenticated as *S. ilicifolium* (TAGGAB D18-A/2024/SPC NO-086) and *Sargassum cinereum* (TAGGAB D18-A/2024/SPC NO-112). The algae were harvested and washed initially with seawater, and then repeatedly rinsed with distilled water to remove epiphytes, sand, and debris. The cleaned biomass was shade-dried at ambient temperature for 4–5 days to conserve the thermolabile constituents and subsequently ground into a fine powder.

Preparation of *S. ilicifolium* extract

For the efficient extraction of bioactive components from the algal biomass, ethanol was used as a suitable solvent as it has the ability to solubilize a wide range of metabolites. Approximately 250 g of dried powder of *S. ilicifolium* was extracted with 2500 mL of ethanol with a sample-to-solvent ratio of 1:10 (w/v) for 48 h with intermittent stirring. After 48 h, Soxhlet extraction was performed. The filtrate was then concentrated under reduced pressure using a rotary evaporator, followed by drying at 40°C to remove residual solvent. This process resulted in 12.5 g of crude ethanolic extract, corresponding to a 5% yield, and which was stored in airtight amber vials at 4°C for further experimental purposes [16-18].

Liquid chromatography-mass spectrometry (LC-MS)

The phytochemical constituents present in the ethanolic extract of *S. ilicifolium* were identified by performing LC-MS analysis. The ethanolic extract was filtered through a 0.2 µm membrane disc, and the filtrate was used for the LC-MS analysis. About 10 µL of the sample was injected into an ultra-performance liquid chromatography (UPLC) system equipped with an ACQUITY UPLC-BEH C18 reverse-phase column. Separation was performed with the mobile phase that comprised formic acid and acetonitrile. Other mass spectrometric parameters were capillary voltage at 4000 V, and nitrogen gas at 35 psi. The mass spectral data acquisition was attained under positive electrospray ionization (ESI). The fragments produced were identified using the available library of molecules, and the phytoconstituents in the extract were detected based on their m/z values.

Isolation of chlorogenic acid (CGA) by column chromatography

The ethanolic extract of *S. ilicifolium* was dried and then dissolved in methanol and adsorbed on the silica gel (100–200 mesh) and allowed to evaporate. The dried material was then loaded onto a silica gel column, which has already been packed with hexane as a mobile phase. Elution was performed with increasing polarity of solvents, namely petroleum ether, ethyl acetate, chloroform, and methanol. Initially, different ratios of petroleum ether and ethyl acetate were used (95:5, 90:10, 85:15, 80:20, 75:25, 70:30, 65:35, 60:40, 50:50, 40:60, 30:70, 20:80, and 10:90) with 100% of ethyl acetate as the final elution. Followed by this, the column is then eluted with an ethyl acetate and chloroform mixture in the same ratio as discussed earlier, with 100 % chloroform in the final elution. Finally, a chloroform and methanol mixture is used for the elution. A total of 104 fractions were obtained at the end, and each fraction was analyzed using thin-layer chromatography (TLC). Fractions 84–92 show similar Rf values, and these fractions were combined and concentrated under reduced pressure to obtain crude material.

The purification of the crude material was carried out by treatment with activated charcoal in the presence of hot ethanol. The solution is filtered, and the filtrate obtained was kept under refrigerated conditions for crystallization. A yellow-colored solid was obtained, which was then subjected to additional structural and spectral characterization studies using ultraviolet-visible spectroscopy (UV-Vis), proton NMR (^{1}H-NMR), and carbon-13 NMR (^{13}C-NMR) spectroscopy, Fourier-transform infrared spectroscopy (FT-IR), and mass spectrometry (MS).

Spectral characterization

FTIR

For FTIR analysis, the sample was prepared by grinding the yellow solid product into fine powder, and nearly 2 mg of the sample was mixed with about 200 mg of potassium bromide (KBr). The mixture was again ground to attain a homogenous mixture with a particle size below 2 µm, which is then compressed in a hydraulic press to a transparent pellet. Perkin Elmer FTIR spectrophotometer 1650 was used for the FTIR analysis, and the readings were measured with the mid-infrared range between 4000 and 400 cm^{-1}.

NMR spectroscopy

The structure of the isolated compound was determined using ^{1}H NMR and ^{13}C NMR spectroscopic studies, and analysis was performed on a Bruker Avance 400 MHz spectrometer, which operates at 400 MHz and 100 MHz, respectively. About 5–20 mg of the sample was dissolved in 0.5–0.7 mL of DMSO and analyzed in the spectrometer. Chemical shifts (δ) were given in parts per million (ppm) relative to TMS as an internal standard.

Mass spectroscopy

The isolated phytoconstituent was dissolved in analytical grade acetonitrile or methanol and filtered through a 0.2 µm membrane filter, and the filtrate was used for mass spectra analysis in an Agilent 5977C Mass spectrometer. Data acquisition and processing were carried out using the manufacturer's software to ensure reproducibility and analytical reliability.

High-performance liquid chromatography (HPLC)

For HPLC analysis, 1 mg of standard CGA was dissolved in 1 mL of methanol, and it was filtered through a polytetrafluoroethylene membrane syringe filter of 0.45 µm pore size. HPLC was performed in a 1200 series Agilent system comprised a binary pump, an autosampler, degassed and a thermostatic column oven, and the chromatogram was generated with the help of EZchrom elite software. 2% acetic acid in water was used for the analysis of the sample. Methanol was used as the mobile phase, which was filtered through a 0.45 µm filter before use. 5 µL of the standard and isolated CGA and spiked sample were injected, and the recordings were measured at the wavelength of 325 nm.

(3-[4,5-dimethylthiazol-2-yl]-2,5 diphenyl tetrazolium bromide) (MTT) assay

The cell viability of the isolated compound in HK-2 cells was assessed using the MTT assay. The cells were initially seeded in a 96-well plate with each well containing the cell density of $\times 10^{3}$ cells/well (100 µL)

and incubated at 37°C in 5% CO_2 for 24 h. Then, these cells were treated with varying concentrations of CGA (50, 100, 200, 400, and 800 µg/mL) and incubated for 24 h at 37°C. Cells without any treatment served as the control group. After incubation, the cells were treated with 20 µL of MTT reagent and allowed to stand for 3–4 h. At the end of incubation, the MTT reagent was discarded, and the purple-colored formazan crystals that were produced by the metabolically active cells were dissolved by the addition of 150 µL of DMSO. The absorbance of each well was measured at 570 nm in a microplate reader. The cell viability percentage was calculated with respect to the control group, and the experiment was performed in triplicate for reproducibility. A graph was plotted with the concentration of the CGA along the x-axis and the percentage of cytotoxicity along the y-axis. From the graph, the IC_{50} value of CGA was calculated [19].

SIRT1 assay (deacetylase assay)

HK-2 cells were cultured under standard conditions and divided into seven experimental groups as indicated in the study design table. After 24 h of treatment, the cells were harvested, washed with ice-cold phosphate-buffered saline, and lysed using the assay buffer supplied with the SIRT1 activity assay kit. The cell lysates were centrifuged at ×12,000 g for 10 min at 4°C to remove cellular debris, and the total protein concentration was quantified using the bicinchoninic acid (BCA) assay.

SIRT1 deacetylase activity was determined using a fluorometric assay according to the manufacturer's instructions. Briefly, 5 µL of protein-normalized cell lysate was incubated with 35 µL of assay buffer, 5 µL of NAD^+ solution, and 5 µL of fluorometric SIRT1 substrate in a 96-well microplate at 37°C for 30 min. Thereafter, 5 µL of developing solution was added to each well, mixed gently, and further incubated at 37°C for 10 min. Fluorescence intensity was measured using a microplate reader at an excitation wavelength of 340 nm and an emission wavelength of 460 nm.

Net fluorescence values were calculated by subtracting blank readings, and SIRT1 activity was determined using a standard curve prepared with a non-acetylated standard. The calculated lysate volumes ensured equal protein input across all experimental groups, allowing accurate normalization of SIRT1 deacetylase activity. Positive controls (resveratrol) were included to validate the assay performance. All steps were performed on ice or at 4°C whenever applicable to minimize protein degradation. All experiments were carried out in triplicate, and the results were expressed as mean±standard deviation (SD) [20].

Molecular docking

Molecular Docking was performed using Auto Dock Vina involving SIRT1 (PDB ID: 5BTR) [21]. First, the crystal structures of the protein were downloaded from the Protein Data Bank and prepared by removing water molecules and co-crystallized ligands, adding polar hydrogens, assigning Gasteiger charges, and saving it in PDBQT format using auto dock tools. The ligand was obtained from the PubChem database, energy minimized using the MMFF94 force field in Avogadro software. Grid boxes for SIRT1 were centered around the NAD^+ or inhibitor binding site, guided by coordinates of the co-crystallized ligands. Docking was performed using AutoDock Vina, and the output gives information on different binding poses and binding affinities. The resulting complexes are analyzed using molecular visualization tools such as PyMOL or Chimera to interpret binding modes, interaction types, and docking scores.

Acute toxicity studies

The animal studies were approved by the Institutional Animal Ethics Committee (DIMHER/IEAC/24-25/13 dated April 25, 2024). Acute oral toxicity of *S. ilicifolium* extract was evaluated following the Organisation for Economic Co-operation and Development (OECD) Test Guideline 423 (acute toxic class method). Healthy adult female rats were used for this experiment. The rats were fasted overnight with water available ad libitum before dosing. The rats were randomly classified into four different treatment groups (Groups I–IV) based on the concentration of the extract being administered. The extract was administered by single oral gavage at doses of 5, 50, 300, and 2000 mg/kg body weight along with untreated rats, which served as a control vehicle. Animals were observed individually at least once within the first 30 min post-dosing, periodically during the first 24 h, and daily for 14 days for any signs of toxicity or mortality. Body weights were recorded before the administration of the extract, on days 7 and 14, and at death. At the end of the observation period, surviving animals were euthanized and subjected to gross necropsy to assess any pathological changes. No mortality or treatment-related toxicity was observed at any dose, and classification of the extract was based on mortality outcomes according to OECD criteria [22].

Animal experimentation

Adult female Wistar rats were used for the experimentation. Female rats are generally more sensitive to nephrotoxic agents (e.g., cyclophosphamide, cisplatin, and gentamicin), showing earlier and more pronounced elevations in serum creatinine, urea, and kidney injury biomarkers. All animals were maintained on a standard pellet diet with free access to tap water and housed under controlled conditions, including a 12-h light/dark cycle and ambient temperature of 20–25°C. Each cage was clearly labelled, and rats were individually identified by a unique code marked on the tail. Following a 1-week acclimatization period to laboratory conditions (Obernier and Baldwin, 2006), animals were randomly allocated into six groups, each containing six rats, and housed in separate stainless-steel cages.

Induction of nephrotoxicity

A total of 42 adult Wistar rats aged 8–12 weeks, weighing between 125 and 165 g, were chosen for the experiment. Cyclophosphamide was selected for the induction of nephrotoxicity as it is known for drug-induced nephrotoxicity. 200 mg/kg of cyclophosphamide was injected through the intraperitoneal route[23].

Experimental design and animal treatment (n=6)

- Group I: Normal control, administered 20 mL/kg of distilled water for 14 days.
- Group II: Cyclophosphamide control (negative control), administered 20 mL/kg distilled water for 14 days plus a single intraperitoneal dose of 200 mg/kg CPM on the 7th day.
- Group III: Positive control administered 200 mg/kg silymarin for 14 days plus CPM on the 7th day.
- Group IV: Treated with 200 mg/kg *S. ilicifolium* for 14 days plus CPM on the 7th day.
- Group V: Treated with 400 mg/kg *S. ilicifolium* extract for 14 days plus CPM on the 7th day.
- Group VI: Treated with 200 mg/kg *S. cinereum* for 14 days plus CPM on the 7th day.
- Group VII: Treated with 400 mg/kg *S. cinereum* for 14 days plus CPM on the 7th day.

Euthanasia of experimental animals

At the completion of the experimental protocol, animals were humanely euthanized by intraperitoneal administration of an overdose of ketamine hydrochloride (100–150 mg/kg body weight). Adequate depth of anesthesia was confirmed by loss of pedal and corneal reflexes, followed by cessation of respiration and cardiac activity. Death was verified before tissue collection. All euthanasia procedures were conducted in accordance with IAEC approval and relevant national and international guidelines for the care and use of laboratory animals.

Tissue collection and processing

The body weights of the rats were measured using an electronic balance before the initiation of treatment on day 0 and again at the end of the treatment period on day 15. For statistical analysis, body weights recorded on days 0 and 15 were considered and expressed as mean±standard error of the mean. This approach ensured accurate monitoring of weight changes associated with treatment or disease

progression. Blood samples were collected immediately from each rat using cardiac puncture under deep anesthesia. The blood was transferred into plain tubes and centrifuged at 5000 rpm for 5 min to separate the serum, which was then stored at 4°C for further analysis.

Serum kidney function biomarker assays

Serum concentrations of uric acid, urea nitrogen, and creatinine were quantified using commercially available assay kits on an automated biochemical analyzer. The serum urea levels were determined following Weatherburn's method, whereas serum creatinine and urea concentrations were estimated according to the procedure described by Ajiboye BO [24]. These assays provided reliable biochemical indices for assessing renal function in the experimental animals.

Renal serum electrolyte levels biomarker assays

Serum electrolyte concentrations were measured using commercial assay kits in accordance with established protocols. Potassium (K+) and sodium (Na+), chloride (Cl–), and calcium (Ca2+) were measured as described in the reported procedure [25]. These assays provided comprehensive insights into electrolyte homeostasis and renal function in the study subjects.

Histopathology

After the collection of blood samples, the rats were euthanized, and both kidneys were surgically excised. Dissection was performed starting from the neck to the pubis, followed by careful opening of the peritoneum using a surgical blade. Kidneys were then gently detached with blunt forceps, placed on aluminum foil, and weighed. The excised kidneys were fixed in 10% neutral buffered formalin for preservation. Following tissue processing, samples were embedded in paraffin wax and sectioned into 5 µm thick slices using a rotary microtome. The tissue sections were mounted on microscope slides, stained with hematoxylin and eosin, and coded for histopathological analysis. Examination under light microscopy focused on assessing tubular necrosis, glomerular congestion, inflammatory cell infiltration, and peritubular congestion, which were evaluated and graded according to established criteria.

Statistical analysis

Statistical comparisons between groups were conducted using one-way analysis of variance, with statistical significance. When significant differences were detected, Tukey's *post hoc* test was applied to identify specific group differences. To evaluate changes in body weight within each group from day 0 to day 15, a paired t-test was utilized. Data were presented as mean±SD and summarized in tables and figures.

RESULTS

LC-MS analysis

The results of the LC-MS analysis of the ethanolic extract of *S. ilicifolium* are given in Table 1. The chromatogram of the extract is given in Fig. 1 with its retention time (RT) and intensity of these phytocompounds. Various alkaloids, glycosides, flavonoids, and polyphenols were found to be present in the extract. Some of the notable phytochemicals include quercetin, kaempferol, luteolin, apigenin, naringenin, ferulic acid, gallic acid, caffeic acid, coumaric acid, etc. Among these phytoconstituents, one of the key phytocompounds found is CGA with m/z of 354.31 and RT of 4.5 min, exhibiting a high degree of similarity in RT and spectral similarity scores, which aligns with the compounds deposited in the libraries.

HPLC analysis

The HPLC chromatograms recorded at 325 nm demonstrate that the isolated sample exhibits a prominent and sharp peak at Rt≈1.916 min with a high area percentage (~96.6%), indicating the presence of a major single component with minimal impurities. The standard chromatogram shows a comparable major peak at Rt≈1.985 min (Area% ~95.2%), confirming the characteristic RT of the reference compound and validating system suitability. Similarly, the spiked standard and test sample display a dominant peak at Rt≈1.915 min (Area% ~95.5%), closely matching the RT of both the isolated sample and standard, thereby confirming compound identity even at lower concentration (Fig. 2).

Characterization of CGA

FTIR

The FTIR spectrum of CGA showed characteristic peaks that define the functional groups in it (Fig. 3). Bands at 3468 cm^{-1} and 3323 cm^{-1} correspond to the O–H stretching vibrations, which indicate the presence of hydroxyl groups of phenolic and carboxylic acid moieties. Peaks at 2968 cm^{-1} and 2842 cm^{-1} confer for the =CH stretching vibrations, corresponding to the vinyl groups in the caffeic acid. A band at 1685 cm^{-1} is for the carbonyl (C=O) stretching of the ester and carboxyl groups. The aromatic C=C stretching displays a peak at 1441 cm^{-1}. In addition, a distinct peak at 1286 cm^{-1} reflects the –CH bending vibrations. This confirms that the isolated compound is CGA (Fig. 4).

Table 1: Compounds identified in the ethanolic extract of *S. ilicifolium* by LC-MS

S. No.	Compound name	Class	Mol. formula	Mol. Wt. (Da)	Peak match (%)	RT
	Alkaloids					
1	Trigonelline	Alkaloid	$C_7H_7NO_2$	137.05	99.4	1.88
2	Salsolinol	Alkaloid	$C_{10}H_{13}NO_2$	179.09	99.5	2.80
3	DL-stachydrine	Alkaloid	$C_7H_{13}NO_2$	143.09	99.0	2.46
4	3-pyridylacetic acid	Alkaloid-related	$C_7H_7NO_2$	137.05	98.9	8.2
5	NP-019811	Alkaloid-like	$C_6H_7NO_2$	125.05	99.8	2.1
	Glycosides					
6	D-(+)-maltose	Glycoside	$C_{12}H_{22}O_{11}$	342.12	99.5	2.88
7	(2R,3R,4S,5S,6R)-oxane-triol derivative	Glycoside	$C_{16}H_{28}O_7$	332.18	99.8	3.18
8	NP-013538	Glycoside-like	$C_{12}H_{16}O_8$	288.08	99.1	3.5
10	Glucoside derivative (reported fragment)	Glycoside	–	–	–	3.7
	Flavonoids					
11	Quercetin	Flavonoid	$C_{15}H_{10}O_7$	302.24	–	6.1
12	Kaempferol	Flavonoid	$C_{15}H_{10}O_6$	286.24	–	9.1
13	Luteolin	Flavonoid	$C_{15}H_{10}O_6$	286.24	–	5.5
14	Apigenin	Flavonoid	$C_{15}H_{10}O_5$	270.24	–	8
15	Naringenin	Flavonoid	$C_{15}H_{12}O_5$	272.25	–	5.5
	Polyphenols					
16	Chlorogenic acid	Polyphenol	$C_{16}H_{18}O_9$	354.31	>99	4.5
17	Caffeic acid	Polyphenol	$C_9H_8O_4$	180.16	–	3.8
18	Ferulic acid	Polyphenol	$C_{10}H_{10}O_4$	194.18	–	4.3
19	Gallic acid	Polyphenol	$C_7H_6O_5$	170.12	–	3.2
20	p-coumaric acid	Polyphenol	$C_9H_8O_3$	164.16	–	4.8

RT: Retention time, LC-MS: Liquid chromatography-mass spectrometry

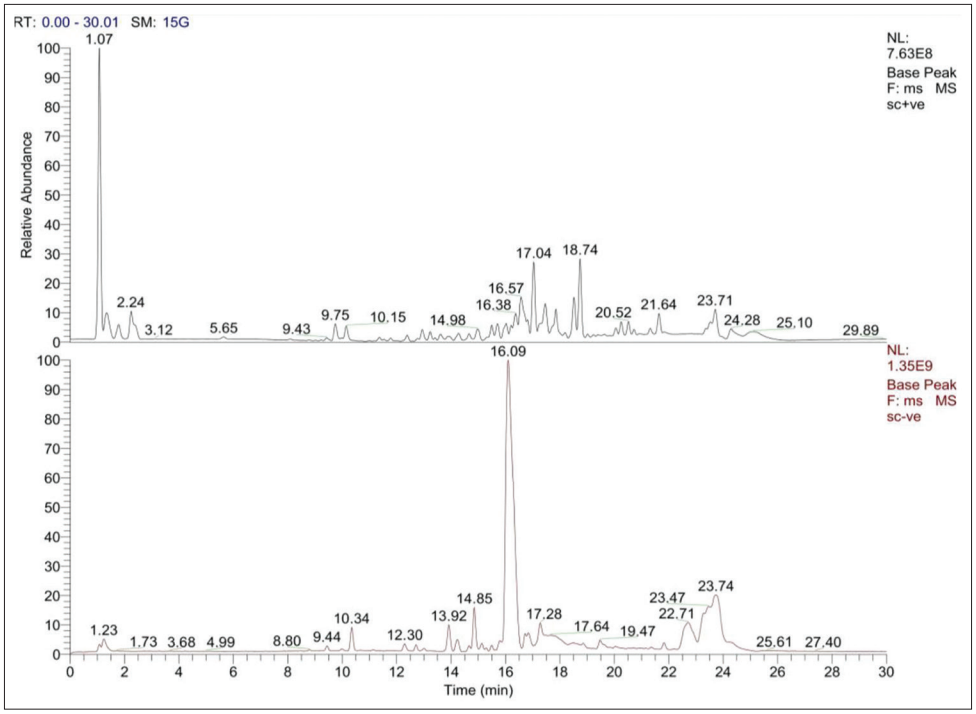

Fig. 1: Liquid chromatography-mass spectrometry chromatogram of *Sargassum ilicifolium*

^{1}H-NMR

^{1}H-NMR (DMSO-*d6*): A downfield singlet at δ 12.40 ppm corresponds to the carboxylic acid proton (-COOH) and two singlets at δ 9.58 and 9.14 ppm, which correspond to aromatic hydroxyl (-OH) protons. The resonance in the aromatic region was between δ 6.97 and 7.43 ppm, which suggests doublets at 7.03 ppm and 7.39–7.43 ppm, and a multiplet at 6.97–6.99 ppm. Quinic acid moiety's protons attached to the hydroxylated carbons were seen at δ 4.76 and 5.08 ppm, whereas additional hydroxyl protons appeared as singlets at δ 3.56, 3.92, and 5.59 ppm for the aliphatic region. Multiplets between δ 1.75 and 2.04 ppm confer for its aliphatic protons in the quinic ring (Fig. 5a-c).

The ^{13}C-NMR spectrum (DMSO-d6): The resonance at δ174.94 ppm corresponds to the carboxylic acid carbon (C7). The aromatic carbons comprising hydroxyl groups were confirmed by the signals δ 165.72, 148.35, 145.56, and 144.96 ppm, which suggest the presence of phenolic hydroxyl groups. Resonance between δ 114.28 and 125.60 ppm suggests the substituted benzene structure. Downfield signals at δ 73.44, 70.89, 70.32, and 68.01 ppm confer for the hydroxylated aliphatic carbons in the quinic acid ring. Resonances at δ 37.20 and 36.19 ppm represented methylene carbons (Fig. 6a-c).

Mass spectroscopy

The molecular weight of the isolated compound was determined by MS (Fig. 7). The mass spectrum showed a molecular ion peak at m/z 355.0, which represents the protonated molecular ion (M+1) of CGA. This aligns with the molecular weight of CGA, which is 354.31 g/mol. Thus, the isolated compound is of high purity and confirmed to be CGA.

Molecular docking

In a molecular docking study, CGA was evaluated for its binding affinity with SIRT1 (PDB ID: 5BTR). CGA exhibited a binding energy of –5.85 kcal/mol, indicative of a weaker interaction at the NAD^+/inhibitor binding site of the deacetylase (Fig. 8a and b; Tables 2 and 3). These suggest that CGA has a higher affinity to SIRT1.

Molecular docking predicted that CGA binds within the NAD^+/inhibitor binding pocket of SIRT1 (–5.85 kcal/mol); however, such structural predictions do not define functional outcomes. Docking provides evidence of ligand–protein interaction but cannot distinguish between activation and inhibition. In contrast, functional analysis by Western blot demonstrated a clear upregulation of SIRT1 protein expression following CGA treatment, which constitutes the primary biological evidence in this study. Thus, functional conclusions are drawn from experimental data rather than *in silico* predictions. The binding of CGA to the SIRT1 catalytic region may modulate enzyme conformation or regulatory interactions without impairing activity.

MTT assay

The cytotoxic effect of CGA in HK-2 cells, analyzed by MTT assay, is given in Figs. 9 and 10. There is an increase in the cytotoxic effect of CGA with an increase in the concentration. 15% of cytotoxicity was seen at 50 µg/mL and up to 80% at 800 µg/mL. The IC_{50} value was found to be 238 µg/mL, and this shows that chlorogenic acid is safe when administered at low doses.

SIRT1 assay

The SIRT1 deacetylase activity assay was conducted to assess the protective effects of plant extracts against cyclophosphamide-induced renal injury in HK-2 cells. The BCA assay showed a highly linear standard curve (R^2=0.9951), ensuring accurate protein normalization. Cyclophosphamide treatment significantly reduced SIRT1 activity (10.80±0.66 µM; ~32–36% of control) compared to the control group (29.33±1.11 µM), indicating oxidative cellular damage and impaired survival signaling.

Treatment with plant extracts produced a dose-dependent restoration of SIRT1 activity. SI showed moderate (low dose) to substantial (high dose) recovery, whereas SC, particularly at high dose (26.80±0.98 µM; ~91% of control), exhibited stronger protective effects. The positive control, resveratrol (20 µM), markedly increased SIRT1 activity (~141% of control), validating assay sensitivity. Overall, the results indicated that plant extracts, especially high-dose SC, significantly mitigated cyclophosphamide-induced suppression of SIRT1 activity, suggesting a nephroprotective effect mediated through activation of the SIRT1 pathway and reduction of oxidative stress (Figs. 11 and 12; Table 4).

Acute toxicity studies show that none of the animals show any observable signs of toxicity. All the animals were well-tolerated up to

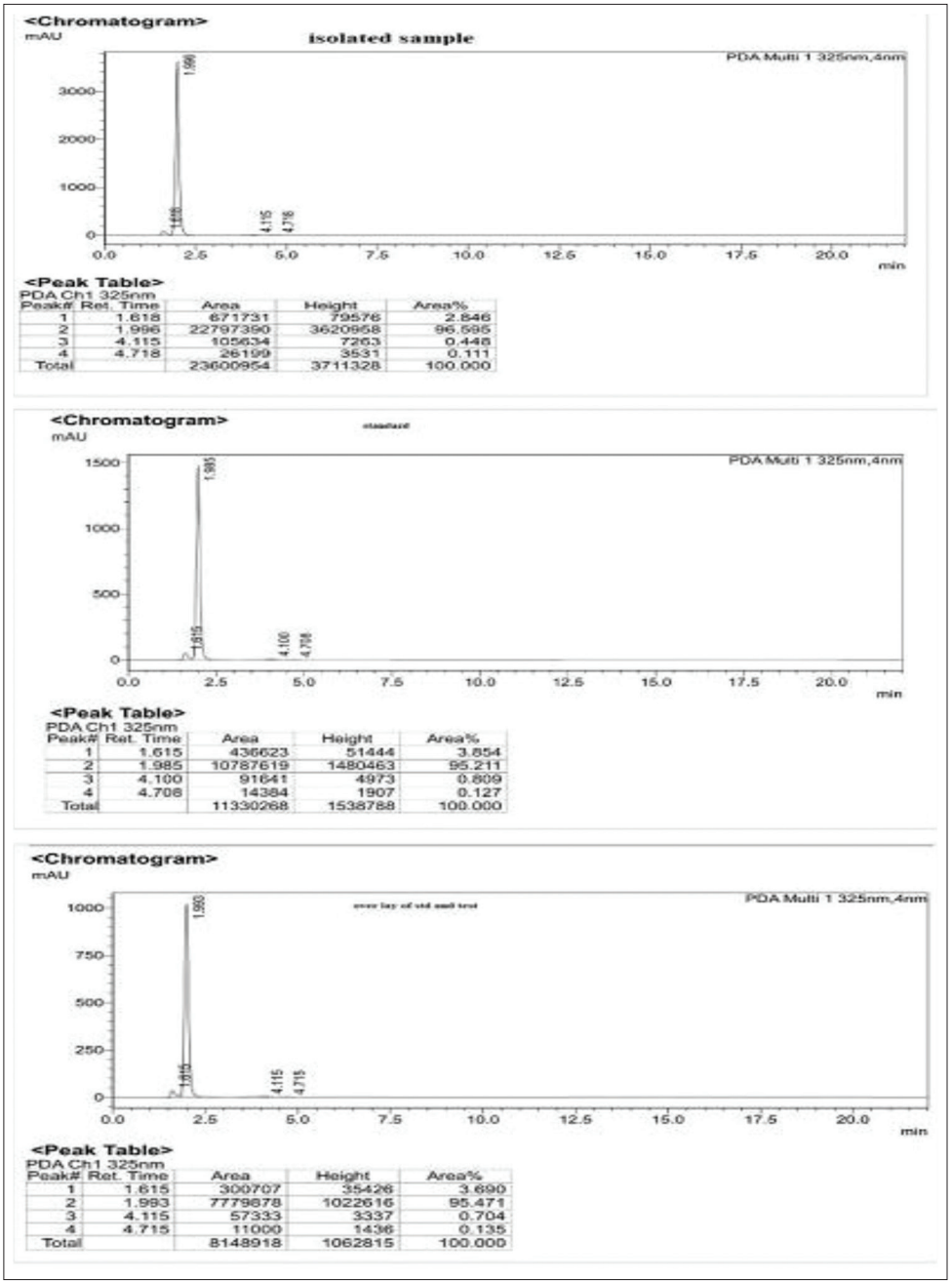

Fig. 2: High performance liquid chromatography overlay chromatogram of isolated, STD chlorogenic acid

a high dose of 2000 mg/kg (Table 5), which suggests that the extract is safe to be administered.

Effect of *S. ilicifolium* on body weight and serum electrolytes

The changes in the body weight of the experimental rats before the onset of treatment and at the end of day 14 were measured and given in Table 6 and Fig. 13. The normal control group has a slight increase in body weight, whereas the CPM-treated group showed a reduction, indicating its nephrotoxic effect. *S. ilicifolium* and *S. cinereum* treated groups have significant weight gain (127.9±0.707 g and 128.9±2.112 g) compared to that of the CPM-only treated group. These results indicate that the weight loss due to nephrotoxicity was restored by *S. ilicifolium* extract, indicating its renoprotective activity.

As given in Figs. 14-17 and Table 7, rats administered with cyclophosphamide show alterations in the level of electrolytes, namely sodium, chloride, potassium, and calcium, which indicates the renal tubular dysfunction and electrolyte imbalance. Rats treated with *S. ilicifolium* extract restored the level of sodium (144.57±3.459 mmol/L), chloride (101.22±0.465 mmol/L), which indicates its renoprotective activity. The levels of potassium and calcium were also shifted closer to the normal range.

Effect of *S. ilicifolium* on renal biomarkers

The renal biomarkers of these groups are given in Table 8 and Figs. 18-20. Administration of cyclophosphamide to the rats shows a drastic increase in the concentration of creatinine (1.57±0.085 mg/dL), uric acid (5.95±0.267 mg/dL), and urea (98.23±3.549 mg/dL) when compared to that of the normal group. In groups IV and V, where 200 mg/kg and 400 mg/kg of *S. ilicifolium* extract administration decreases these renal biomarkers, with the high dose treated group having better efficacy, in which the concentration of serum creatinine, uric acid, and urea were 0.56±0.052 mg/dL, 2.01±0.128 mg/dL, and 29.12±3.296 mg/dL. Rats in groups VI and VII treated with *S. cinereum* exhibited similar reduction

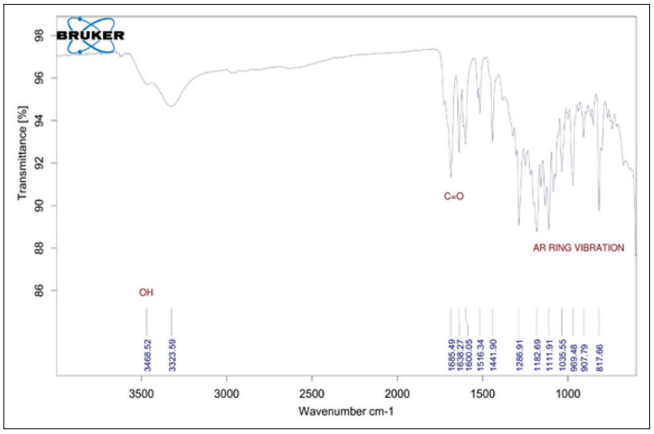

Fig. 3: IR spectrum of chlorogenic acid

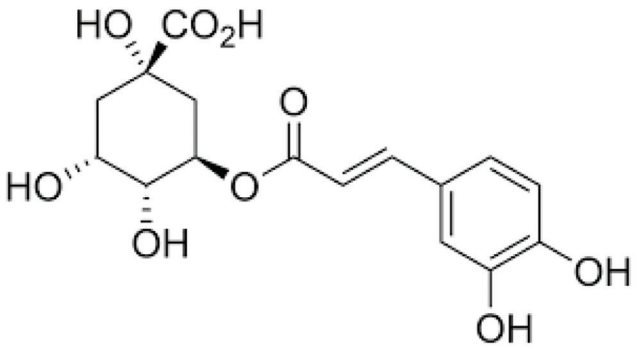

Fig. 4: Structure of chlorogenic acid

in renal biomarkers, serum creatinine (0.56±0.069 mg/dL), uric acid (2.00±0.359 mg/dL), and urea (28.12±4.490 mg/dL) levels.

Histopathological changes

The histopathological changes in the renal tissues of healthy and cyclophosphamide-induced nephrotoxicity rats are given in Fig. 21. In Group II rats, vacuolar degeneration, necrosis, and swelling in the renal tubules were observed due to the toxic effect of CPM. In Group IV and V rats, which were treated with a low dose of *S. ilicifolium* extract, the intensity of glomerular and tubular degeneration was reduced, and at a high dose, the structure and architecture of the renal tubules were minimal, which suggests its renoprotective activity against CPM-induced renal injury. However, rats in groups VI and VII treated with low and high doses of *S. cinereum* extract showed a decrease in the pathological changes in the architecture of renal tubules. Group III rats treated with silymarin show no pathological alterations in the renal tissues.

DISCUSSION

The present study focused on the extraction, identification, and isolation of bioactive constituents from the marine brown alga *S. ilicifolium*, with particular emphasis on CGA due to its known nephroprotective potential. Fresh algal samples were collected from the intertidal zone of Rameswaram, Tamil Nadu (9.2876° N, 79.3173° E), an ecologically rich coastal region known for diverse marine flora. Proper taxonomic authentication ensured the reliability of the biological material used for phytochemical investigation.

Ethanol was selected as the extraction solvent because of its efficiency in dissolving a broad spectrum of polar and moderately polar phytoconstituents. Extraction of 250 g of dried algal powder with 2500 mL of ethanol (1:10 w/v) yielded 12.5 g of crude extract, corresponding to a 5% extraction yield, indicating effective recovery of soluble metabolites. The use of shade drying and controlled temperature conditions during solvent removal helped preserve thermolabile compounds, which is critical for maintaining biological activity.

LC-MS analysis of the ethanolic extract revealed the presence of multiple phytochemicals based on their characteristic m/z values under positive ESI mode. The detection of CGA among these constituents confirmed the suitability of *S. ilicifolium* as a marine source of phenolic compounds. LC-MS profiling provided molecular-level evidence supporting further purification efforts.

Isolation of CGA was successfully achieved through silica gel column chromatography using a gradient elution system with increasing solvent polarity. A total of 104 fractions were collected, and TLC analysis enabled effective monitoring of compound separation. Fractions 84–92, which exhibited similar Rf values, were pooled, indicating the presence of a single predominant compound. Subsequent purification using activated charcoal and recrystallization from hot ethanol yielded a yellow crystalline solid, suggesting a high degree of purity.

Structural confirmation of the isolated compound was accomplished using multiple spectroscopic techniques, including UV-Vis, FT-IR, ^{1}H-NMR, ^{13}C-NMR, and MS. The combined spectral data were consistent with the characteristic functional groups and molecular framework of CGA, thereby validating the isolation procedure. Overall, the results demonstrate that *S. ilicifolium* is a viable marine source of CGA and highlight the effectiveness of ethanol extraction followed by chromatographic purification.

The characterization of CGA was performed using FTIR, ^{1}H-NMR, ^{13}C-NMR, and MS analyses. The FTIR spectrum exhibited peaks corresponding to hydroxyl groups (3468 and 3323 cm^{-1}), vinyl =CH stretches (2968 and 2842 cm^{-1}), carbonyl (C=O) group at 1685 cm^{-1}, aromatic double bonds at 1441 cm^{-1}, and –CH bending at 1286 cm^{-1}, which is similar to the already reported literature studies. The ^{1}H-NMR and ^{13}C-NMR resonances' chemical shifts match those of CGA. MS revealed the molecular ion peak at m/z 355.0 (M+1), validating compound identity and purity [26].

Docking analysis

SIRT1 protein plays a major role in the regulation of metabolic stress, thereby preventing oxidative stress, apoptosis, and inflammation in renal cells. Persistent hyperglycemia in diabetic nephropathy conditions affects the expression of SIRT1 protein, thereby resulting in the onset of renal injury. CGA from *S. ilicifolium* increases the expression of SIRT1, thereby mitigating the onset of renal injury. SIRT1 activation deacetylates FOXO and PGC-1α, thereby increasing the anti-oxidant mechanism and mitochondrial biogenesis and inhibiting the NF-κB signaling. The docking interaction of SIRT1 with CGA shows a binding energy of –5.85 kcal/mol. The interaction analysis revealed that CGA is stabilized by Glu214, Asp292, Asp298, Ala295, Gln294, Thr209, Lys444, Arg446, Phe414, Pro212, and Val445 at SIRT1 protein. These residues, through hydrogen bonds and polar or hydrophobic contacts, anchor the ligand within the binding site. This suggests that CGA exhibits its interaction with SIRT1. Although molecular docking analysis suggests an interaction between CGA and SIRT1, it is important to note that direct binding of a ligand to the catalytic active site of an enzyme is typically associated with inhibitory effects rather than activation. Enzymatic activation of SIRT1 is more commonly achieved through allosteric modulation or indirect mechanisms that enhance enzyme conformation, substrate affinity, or cellular NAD^{+} availability. Therefore, the observed nephroprotective effects of CGA are unlikely to result from classical active-site binding and instead may involve allosteric regulation of SIRT1 or upregulation of its expression and activity under oxidative stress conditions. This interpretation aligns with established mechanisms of SIRT1 activation and avoids mechanistic overstatement based solely on docking data.

***In vitro* studies MTT assay**

The cytotoxic effect of CGA on HK-2 human renal proximal tubular epithelial cells was quantitatively evaluated using the MTT assay, and

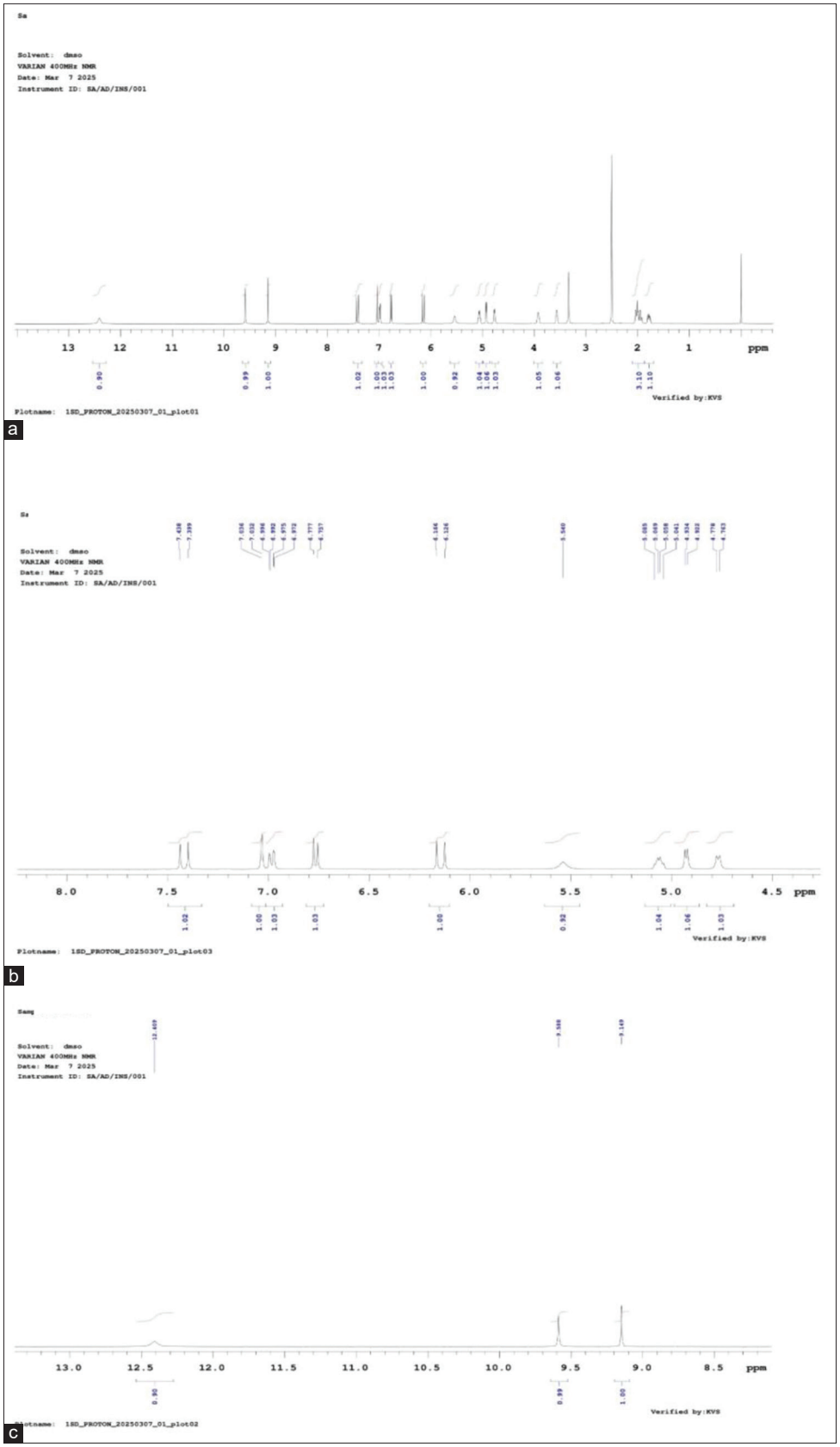

Fig. 5: (a-c) proton nuclear magnetic resonance spectrum of chlorogenic acid

the dose–response relationship was analyzed using a variable-slope nonlinear regression model. The analysis revealed a logIC_{50} value of 2.376, corresponding to an IC_{50} of 237.6 μg/mL, indicating moderate cytotoxicity of CGA toward HK-2 cells at higher concentrations.

The reliability of the IC_{50} value was supported by narrow 95% confidence intervals (223.2–253.0 μg/mL), reflecting good precision of the fit. The Hill slope of 1.188 suggests a concentration-dependent response with a moderately steep transition from viable to non-viable cells, indicating

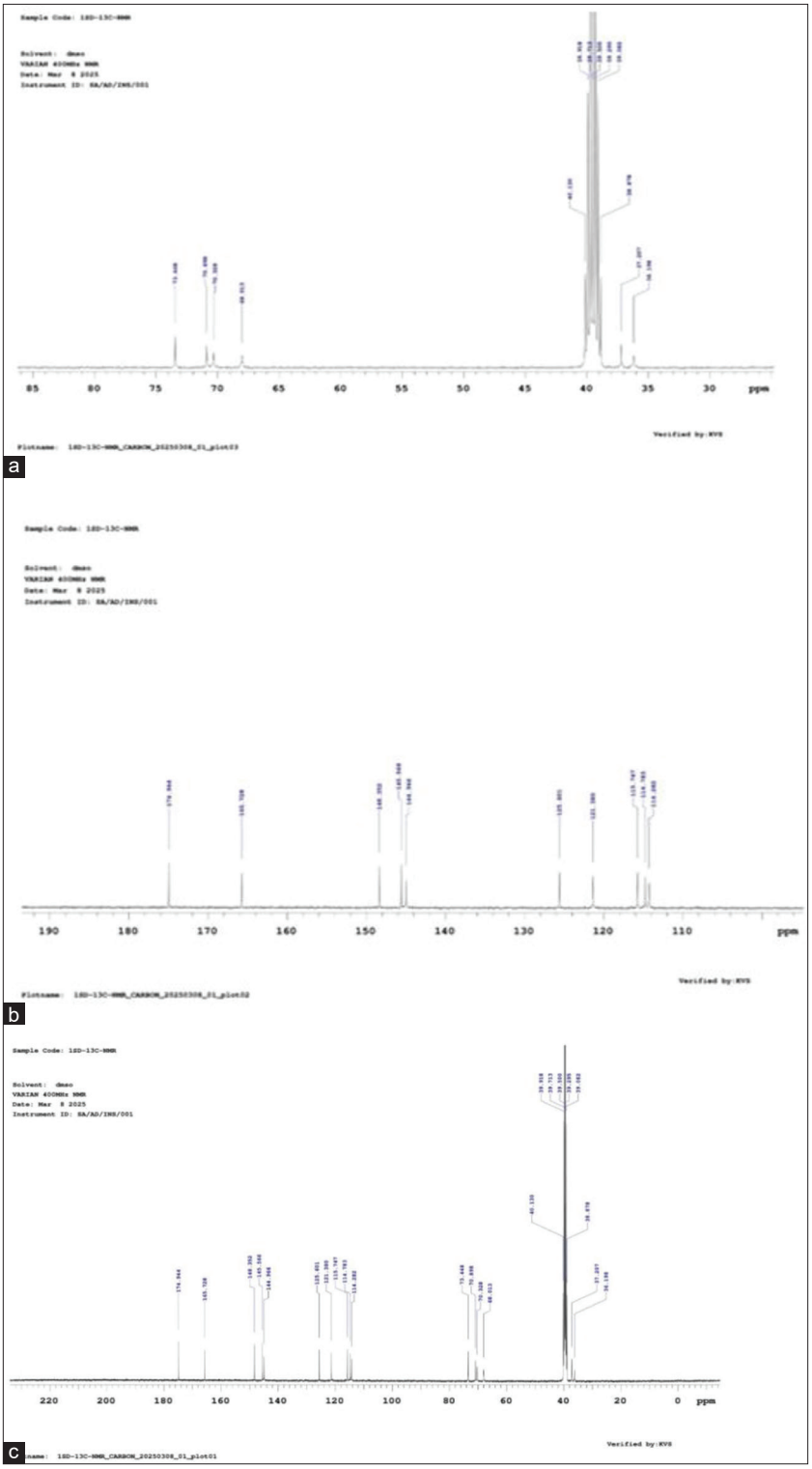

Fig. 6: (a-c) Carbon-13 nuclear magnetic resonance spectrum of chlorogenic acid

cooperative cellular sensitivity to increasing concentrations of CGA. The goodness-of-fit parameters further validated the model, with a high R^2 value of 0.9904, a low standard error (Sy.x=2.588), and acceptable residual variance (absolute sum of squares=87.10), confirming excellent agreement between experimental and predicted values.

Importantly, concentrations below the IC_{50} – particularly ≤100 µg/mL – exhibited minimal cytotoxicity, consistent with earlier dose-dependent observations. This indicates that CGA is well tolerated by renal epithelial cells at lower concentrations, supporting its suitability for nephroprotective studies. Conversely, concentrations approaching or exceeding the IC_{50} produced significant loss of cell viability, highlighting the importance of dose optimization.

Overall, the MTT assay results establish a clear cytotoxic threshold for CGA in HK-2 cells and provide a strong experimental basis for selecting subcytotoxic concentrations (<200 µg/mL) in subsequent mechanistic studies.

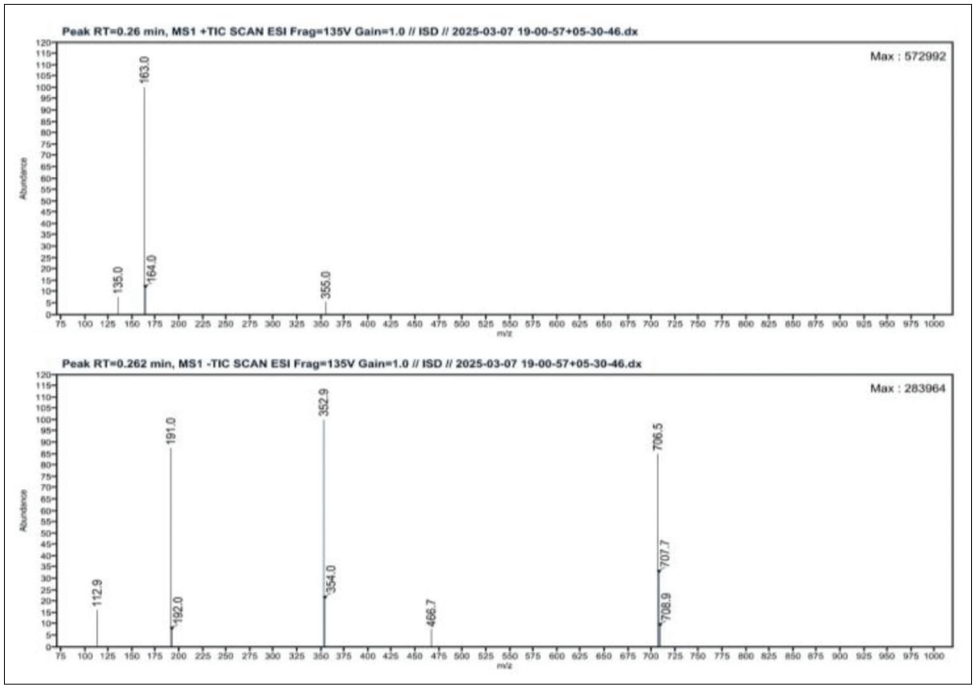

Fig. 7: Mass spectrum of chlorogenic acid

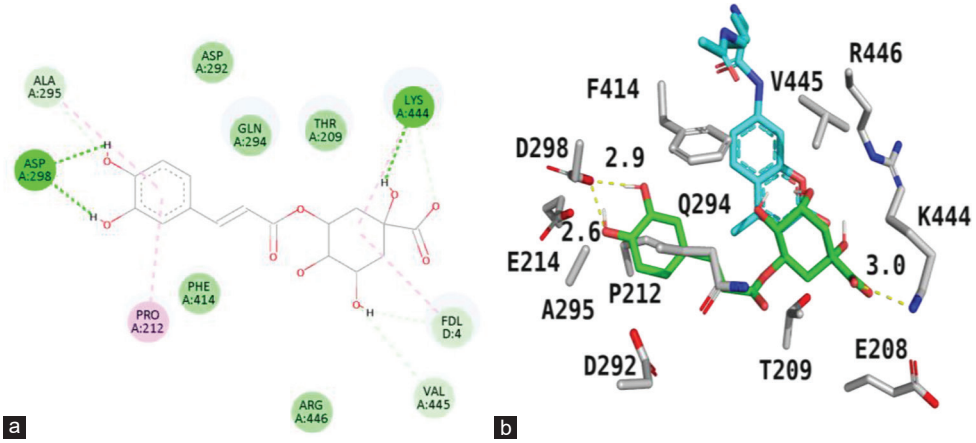

Fig. 8: (a and b) 2D and 3D interaction between chlorogenic acid and the binding site residues of human Sirtuin 1 (PDB ID:5BTR)

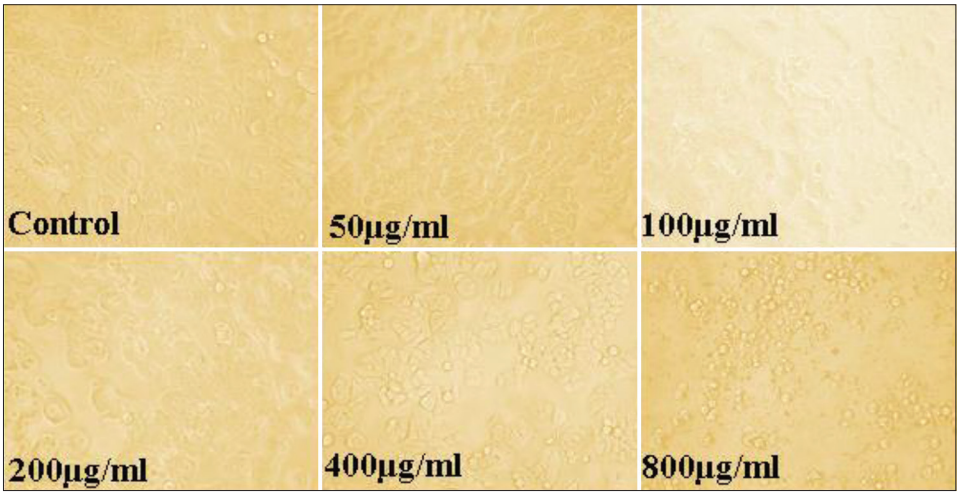

Fig. 9: Cell viability of different concentrations of chlorogenic acid in HK-2 cells

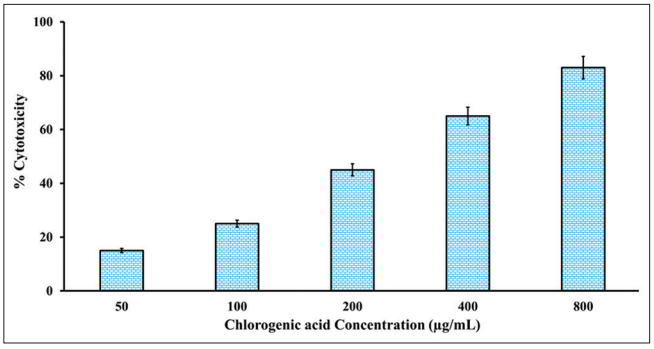

Fig. 10: Cytotoxicity percentage of different concentrations of chlorogenic acid in HK-2 cells

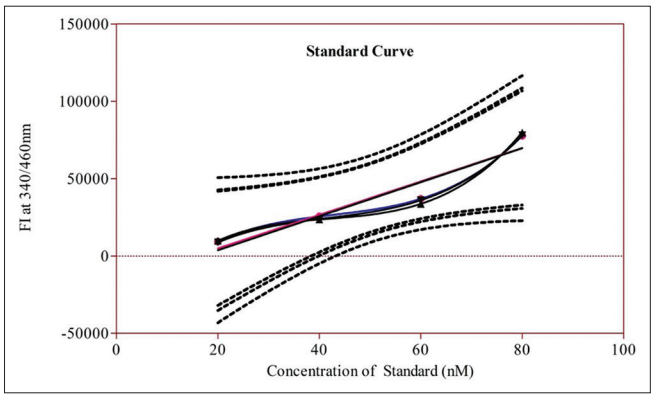

Fig. 11: STD calibration graph of Sirtuin 1 deacetylase assay

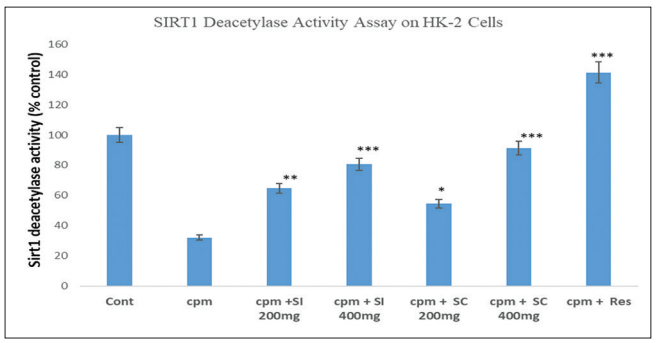

Fig. 12: Bar graph of SIR T1 deacetylase assay. Values are expressed as mean±standard deviation (n=3) asterisk mark superscripts indicate statistical significance: *p<0.05; **p<0.01; ***p<0.001 versus negative control

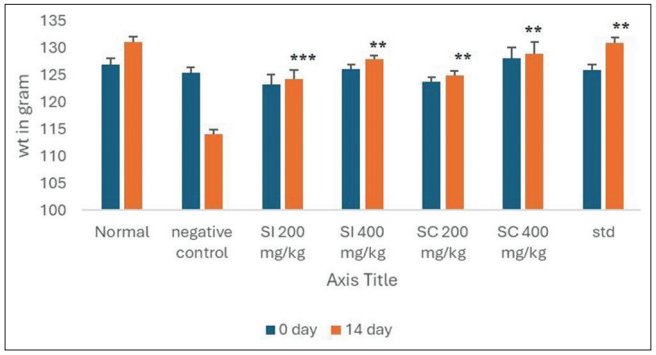

Fig. 13: Change in body weight between different groups. Values are expressed as mean±standard deviation (n=6) asterisk mark superscripts indicate statistical significance: **p<0.01; ***p<0.001 versus negative control

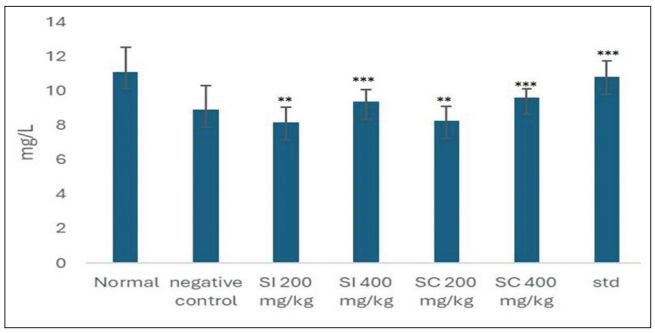

Fig. 14: Change in calcium concentration between different groups. Values are expressed as mean±standard deviation (n=6) asterisk mark superscripts indicate statistical significance: **p<0.01; ***p<0.001 versus negative control

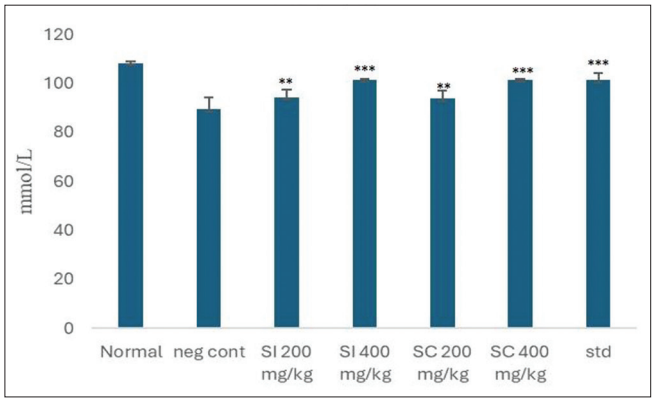

Fig. 15: Change in chloride concentration between different groups. Values are expressed as mean±standard deviation (n=6) asterisk mark superscripts indicate statistical significance: **p<0.01; ***p<0.001 versus negative control

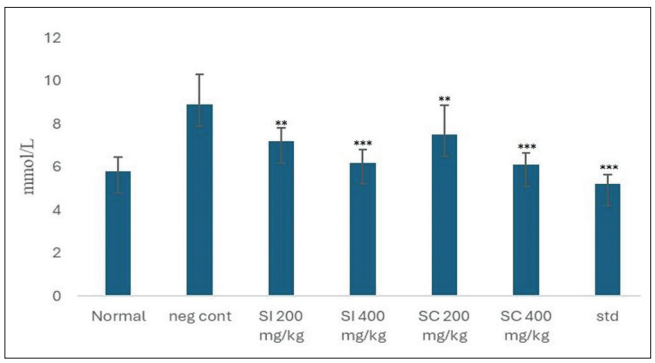

Fig. 16: Change in potassium concentration between different groups. Values are expressed as mean±standard deviation (n=6) asterisk mark superscripts indicate statistical significance: **p<0.01; ***p<0.001 versus negative control

Acute toxicity studies

The acute oral toxicity study demonstrated that the extract is well-tolerated up to a dose of 2000 mg/kg, with no mortality observed across all experimental groups. The estimated LD_{50} >2000 mg/kg classifies the extract as relatively non-toxic according to OECD acute toxicity guidelines, supporting its safety for further pharmacological investigations. These findings provide a critical foundation for dose selection in subsequent *in vivo* anti-diabetic and nephroprotective studies, ensuring that administered doses remain within a safe range.

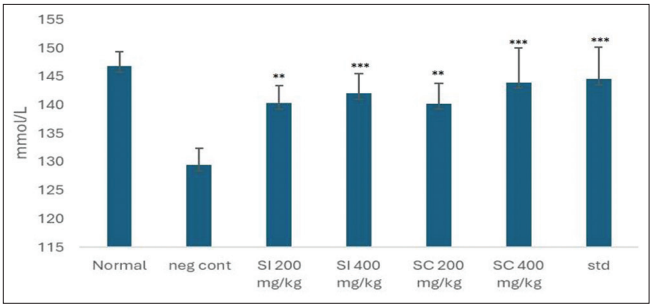

Fig. 17: Change in sodium concentration between different groups. Values are expressed as mean±standard deviation (n=6) asterisk mark superscripts indicate statistical significance: **p<0.01; ***p<0.001 versus negative control

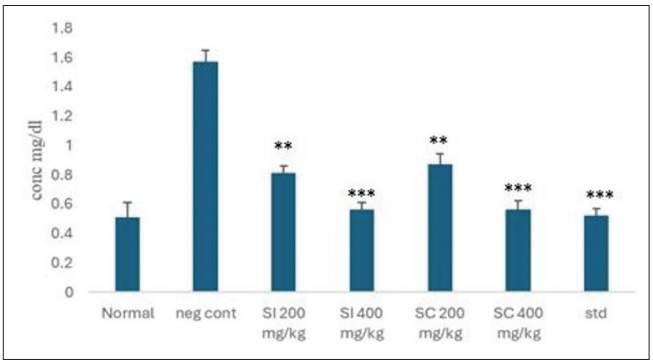

Fig. 18: Change in serum creatinine concentration between different groups. Values are expressed as mean±standard deviation (n=6) asterisk mark superscripts indicate statistical significance: **p<0.01; ***p<0.001 versus negative control

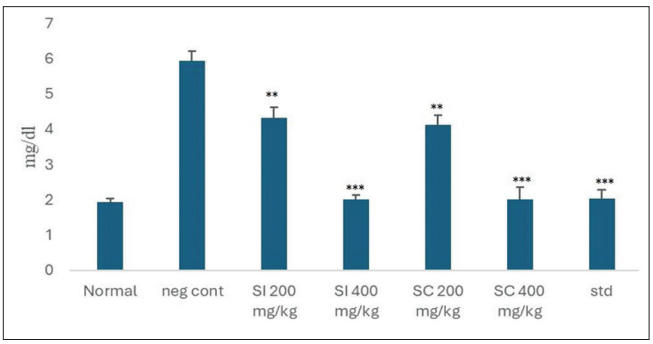

Fig. 19: Change in uric acid concentration between different groups. Values are expressed as mean±standard deviation (n=6) asterisk mark superscripts indicate statistical significance: **p<0.01; ***p<0.001 versus negative control

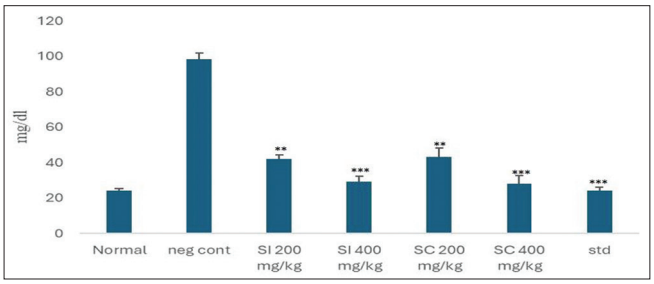

Fig. 20: Change in urea concentration between different groups. Values are expressed as mean±standard deviation (n=6) asterisk mark superscripts indicate statistical significance: **p<0.01; ***p<0.001 versus negative control

Table 2: Molecular docking of chlorogenic acid with Sirtuin 1 protein

Target (PDB ID)	Compound (Pubchem)	Name of the compound	Binding energy (kcal/mol)	Predicted inhibitory constant value
human SIRT1 (PDB ID: 5BTR)	1794427	Chlorogenic acid	−5.85	51.86 µM

Table 3: Summary of molecular interactions between chlorogenic acid and the binding site residues of human Sirtuin 1

S. No.	Interaction type	Binding residues
1	Hydrophobic interactions	F414, V445, P212, A295
2	Hydrophilic interaction	E214, D292, D298, Q294, E208, K444
3	Hydrogen bond interactions	E214, D298, K444
4	π-π interactions	F414 (with aromatic ring of ligand)
5	Cation-π interactions	K444, R446 (likely candidates)

Table 4: SIRT1 deacetylase assay

Study groups	Mean±standard deviation (n=3)
Normal control	100.0±3.8
Cyclophosphamide (CPM) induced renal injury negative control	32.16477+±2.2
CPM+low dose SI	64.7976±1.4**
CPM+high dose SI	80.60629±2.6***
CPM+high dose SC	91.36235±3.4*
CPM+low dose SC	54.4952±2.9***
CPM+20µm Resveratol	141.2504±1.8***

Data are expressed as mean±standard deviation (n=3). Statistical analysis was performed using one-way analysis of variance followed by Dunnett's multiple comparison test, with the negative control (cyclophosphamide-treated group) as the reference. *p<0.05; **p<0.01; ***p<0.001 versus negative control (CPM)

Table 5: Acute toxicity studies in rats (n=3) with varying doses of *Sargassum ilicifolium* extract

Group no	Dose no (mg/kg)	Mortality
Group-I	5 (mg/kg)	0 of 3
Group-II	50 (mg/kg)	0 of 3
Group-III	300 (mg/kg)	0 of 3
Group-IV	2000 (mg/kg)	0 of 3

Table 6: The mean weight difference of rats on day 0 and day 14

S. No.	Body weight on day 0 Mean±SD	Body weight on day 14 Mean±SD
Normal control	126.9±1.176	131.0±1.124
CP control (negative control)	125.4±0.924	114.02±0.895
Positive control (STD control)	125.8±1.095^{ns}	130.9±0.964**
200 mg/kg SI	129.2±1.762^{ns}	124.2±1.729***
400 mg/kg SI	126.1±0.743^{ns}	127.90±0.707**
200 mg/kg SC	124.7±0.835^{ns}	123.9±0.846**
400 mg/kg SC	128.0±1.997^{ns}	128.9±2.112**

Values are expressed as mean±standard deviation (SD) (n=6). Statistical analysis was performed using one-way analysis of variance followed by a multiple comparison test, with all treatment groups compared against the negative control. Superscripts indicate statistical significance: ^{ns}p>0.05; **p<0.01; ***p<0.001 versus negative control

Table 7: Concentration of serum sodium, potassium, calcium, and chloride levels between different groups

S. No.	Sodium (mmol/L) mean±SD	Potassium (mmol/L) mean±SD	Calcium (mg/L) mean±SD	Chloride (mmol/L) mean±SD
Normal control	146.8±2.556	5.8±0.679	11.1±1.441	108.25±0.881
CP control (negative control)	129.4±3.024	8.9±1.436	8.9±1.396	89.30±4.936
STD control (Positive control)	144.5**±5.652	5.2***±0.438	10.8***±0.956	101.23***±2.772
200 mg/kg SI	140.26**±3.118	7.2**±0.637	8.15**±0.912	94.32**±3.103
400 mg/kg SI	142.02***±3.459	6.2***±0.607	9.36***±0.720	101.52***±0.465
200 mg/kg SC	140.23**±3.560	7.5***±1.350	8.25**±0.840	93.78**±3.153
400 mg/kg SC	143.92***±6.124	6.1***±0.540	9.62***±0.493	101.45***±0.509

Values are expressed as mean±standard deviation (SD) (n=6). Statistical analysis was performed using one-way analysis of variance followed by a multiple comparison test, with all treatment groups compared against the negative control. Asterisk mark superscripts indicate statistical significance: **p<0.01; ***p<0.001 versus negative control

Table 8: Concentration of serum creatinine, uric acid, and urea levels between different Groups

S. No.	Serum creatinine levels (mg/dL) mean±SD	Uric acid levels (mg/dL) mean±SD	Urea levels (mg/dL) mean±SD
Normal control	0.51±0.101	1.93±0.104	23.99±1.331
CPM (negative control)	1.57±0.085	5.95±0.267	98.23±3.549
Positive control (STD control)	0.52***±0.054	2.03***±0.263	24.23***±1.678
200 mg/kg SI	0.81**±0.056	4.32**±0.315	42.02**±2.422
400 mg/kg SI	0.56***±0.052	2.01***±0.128	29.12***±3.296
200 mg/kg SC	0.87**±0.075	4.12**±0.282	43.12**±4.974
400 mg/kg SC	0.56***±0.069	2.00***±0.359	28.12***±4.490

Values are expressed as mean±standard deviation (SD) (n=6). Statistical analysis was performed using one-way analysis of variance followed by a multiple comparison test, with all treatment groups compared against the negative control. Superscripts indicate statistical significance: **p<0.01; ***p<0.001 versus negative control

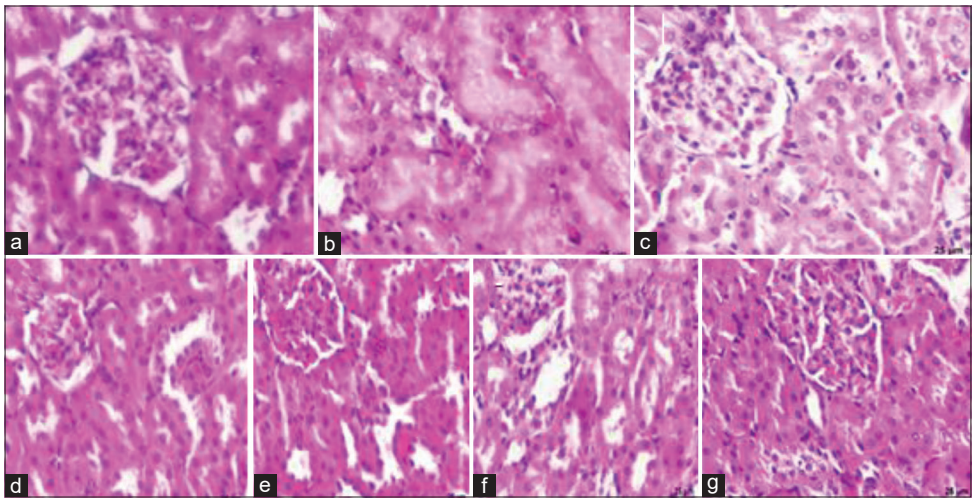

Fig. 21: (a) Control group showing normal glomeruli and tubules with no significant pathological changes. (b) Toxic group (cyclophosphamide) showing Vacuolar degeneration, tubular, multifocal, moderate. (c) Standard group (silymarin) showing normal glomeruli and tubules with no significant pathological changes. (d) Low dose group of *Sargassum ilicifolium* extract showing Vacuolar degeneration, tubular, multifocal, mild. (e) High dose group of *S. ilicifolium* extract showing Vacuolar degeneration, tubular, multifocal, minimal. (f) Low dose group of *Sargassum cinereum* extract showing Vacuolar degeneration, tubular, multifocal, minimal. (g) High dose group of *S. cinereum* extract showing normal glomeruli and tubules with no significant pathological changes

Nephroprotective studies

Body weight measurement

In the CPM (cyclophosphamide) control group, body weight significantly decreased from 125.4±0.924 g on day 0 to 114.02±0.895 g on day 14, reflecting renal toxicity and systemic stress. In contrast, the normal control group showed a modest increase in body weight (126.9±1.176 g → 131.0±1.124 g), indicating normal growth and health.

Administration of SI and SC significantly attenuated the CPM-induced weight loss in a dose-dependent manner. The higher doses of both SI (400 mg/kg) and SC (400 mg/kg) demonstrated substantial protection, with body weights of 127.9±0.707 g and 128.9±2.112 g, respectively, closely approaching the normal and standard control groups. These results suggest that both SI and SC exert protective effects against CP-induced nephrotoxicity, with enhanced efficacy at higher doses.

Biochemical parameters

Cyclophosphamide (CPM) administration in the negative control group led to significant renal impairment, as indicated by elevated serum creatinine, uric acid, and urea, consistent with nephrotoxicity characterized by glomerular and tubular damage. These findings are in agreement with previous reports demonstrating that CPM induces

oxidative stress, inflammation, and apoptosis in renal tissue, leading to compromised renal function and elevated biochemical markers.

Treatment with 200 mg/kg SI or SC significantly reduced these renal biomarkers, while the higher dose (400 mg/kg) restored values closer to normal, demonstrating a dose-dependent nephroprotective effect. This aligns with previous studies showing that CGA and polyphenol-rich extracts can mitigate drug-induced nephrotoxicity by reducing oxidative stress, suppressing inflammation, and improving renal function.

Mechanistically, CGA exerts nephroprotection through restoration of SIRT1 expression in renal tubular cells, which enhances anti-oxidant defense, reduces apoptosis, and improves glucose handling [27]. The observed biochemical improvements in creatinine, urea, and uric acid are consistent with these cellular mechanisms, confirming that the extract and CGA not only prevent structural renal damage but also restore functional renal biomarkers.

Collectively, these results corroborate previous literature and highlight the potential of CGA and polyphenol-rich extracts as natural nephroprotective agents in models of chemically-induced renal injury, emphasizing the importance of dose optimization to maximize therapeutic benefits [28].

Cyclophosphamide (CPM) administration in the negative control group caused significant electrolyte disturbances, including reduced sodium (129.4±3.024 mmol/L) and chloride (89.30±4.936 mmol/L) and elevated potassium (8.9±1.436 mmol/L). These alterations reflect CP-induced renal tubular injury, impaired glomerular filtration, and dysregulation of renal ion transport mechanisms, consistent with prior reports showing that nephrotoxic agents disrupt electrolyte homeostasis.

Treatment with 200 mg/kg SI or SC significantly improved electrolyte levels ($p<0.01$), and 400 mg/kg restored electrolytes close to normal ($p<0.001$), demonstrating a dose-dependent nephroprotective effect. These improvements are likely mediated by CGA, which has been reported to mitigate oxidative stress, reduce tubular apoptosis, and preserve renal transporter function, thereby maintaining electrolyte balance.

Previous studies support these findings: Wang *et al.* (2019) [28] showed that CGA restored renal tubular function in high-glucose-induced HK-2 cell injury by enhancing SIRT1 expression, whereas Zhang *et al*. demonstrated that CGA alleviates renal fibrosis and tubular dysfunction, contributing to the normalization of renal biomarkers and electrolyte homeostasis. Moreover, Bao *et al*. reported that CGA prevents nephropathy by modulating oxidative stress and inflammation through Nrf2/HO-1 and NF-κB pathways, further supporting its role in maintaining ionic balance in renal injury [29,30].

Collectively, these findings indicate that SI and SC exert comprehensive nephroprotective effects, not only improving renal biomarkers and body weight but also correcting CP-induced electrolyte imbalances. The dose-dependent efficacy emphasizes the importance of optimizing therapeutic dosing to achieve maximal renal protection while minimizing potential toxicity.

Cyclophosphamide (CPM) administration caused moderate tubular epithelial damage, while silymarin preserved normal renal structure. Treatment with SI and SC showed dose-dependent protection: low doses caused mild or minimal lesions, whereas high-dose SC fully restored normal glomerular and tubular architecture, indicating complete histological recovery.

CONCLUSION

This study highlights the nephroprotective potential of *S. ilicifolium*, attributed primarily to CGA, one of its major bioactive constituents. The protective mechanism involves the upregulation of SIRT1, a pivotal regulator of cellular stress responses and renal homeostasis. Administration of the extract led to significant improvements in renal biomarkers and serum electrolyte profiles, alongside preservation of kidney histoarchitecture. These outcomes underscore the therapeutic promise of *S. ilicifolium* in ameliorating CPM induced renal injury, with CGA-mediated SIRT1 modulation emerging as a central mechanistic axis.

ACKNOWLEDGMENT

I would like to express my heartfelt appreciation to Dr.Rahul Ingle, Professor, Department of Pharm Chemistry, Datta Meghe College of Pharmacy, DMIHER (DU), Sawangi, Wardha, for his professional guidance and assistance throughout the studies.

AUTHOR'S CONTRIBUTIONS

Rahul Ingle designed the work, Chandupatla Ramya carried out the experimental work, analysis, and interpretation of data, statistical analysis of data, Mrs. Reena and Mariappan contributed to the research article drafting, and revised the article.

CONFLICTS OF INTEREST

No conflicts of interest.

SOURCE OF FUNDING

Nil.

REFERENCES

1. Lewington AJ, Cerdá J, Mehta RL. Raising awareness of acute kidney injury: A global perspective of a silent killer. Kidney Int. 2013;84(3):457-67. doi: 10.1038/ki.2013.153, PMID 23636171
2. Mehta RL, Cerdá J, Burdmann EA, Tonelli M, García-García G, Jha V. International Society of Nephrology's 0by25 initiative for acute kidney injury (zero preventable deaths by 2025): A human rights case for nephrology. Lancet. 2015;385(9987):2616-43. doi: 10.1016/s0140-6736(15)60126-x, PMID 25777661
3. Chawla LS, Bellomo R, Bihorac A, Goldstein SL, Siew ED, Bagshaw SM. Acute kidney disease and renal recovery: Consensus report of the Acute Disease Quality Initiative (ADQI) 16 Workgroup. Nat Rev Nephrol. 2017;13(4):241-57. doi: 10.1038/nrneph.2017.2, PMID 28239173
4. Levey AS. Defining AKD: The spectrum of AKI, AKD, and CKD. Nephron. 2022;146(3):302-5. doi: 10.1159/000516647, PMID 34167119
5. He W, Wang Y, Zhang MZ, You L, Davis LS, Fan H. Sirt1 activation protects the mouse renal medulla from oxidative injury. J Clin Invest. 2010 Apr 01;120(4):1056-68. doi: 10.1172/jci41563
6. Kitada M, Kume S, Takeda-Watanabe A, Kanasaki K, Koya D. Sirtuins and renal diseases: Relationship with aging and diabetic nephropathy. Clin Sci (Lond). 2013 Feb 01;124(3):153-64. doi: 10.1042/cs20120190
7. Chen HH, Zhang YX, Lv JL, Liu YY, Guo JY, Zhao L. Role of sirtuins in metabolic disease-related renal injury. Biomed Pharmacother. 2023 May 1;161:114417. doi: 10.1016/j.biopha.2023.114417
8. Kume S, Haneda M, Koya D. SIRT1 in renal disease: Mechanisms and therapeutic potential. J Mol Med. 2012;90(8):907-15.
9. Hasegawa K, Wakino S, Yoshioka K, Tatematsu S, Hara Y, Minakuchi H. Kidney-specific overexpression of Sirt1 protects against acute kidney injury by retaining peroxisome function. J Biol Chem. 2010;285(17):13045-56. doi: 10.1074/jbc.M109.067728, PMID 20139070
10. Morigi M, Perico L, Benigni A. Sirtuins in renal health and disease. J Am Soc Nephrol. 2018;29(7):1799-809. doi: 10.1681/asn.2017111218, PMID 29712732
11. Gao LI, Zhong X, Jin J, Li J, Meng XM. Potential targeted therapy and diagnosis based on novel insight into growth factors, receptors, and downstream effectors in acute kidney injury and acute kidney injury-chronic kidney disease progression. Signal Transduct Target Ther. 2020 Feb 14;5(1):9. doi: 10.1038/s41392-020-0106-1, PMID 32296020
12. Lameire N, Kellum JA, KDIGO AK Guideline Work Group. Contrast-induced acute kidney injury and renal support for acute kidney injury:

A KDIGO summary (Part 2). Crit Care. 2013 Feb 04;17(1):205. doi: 10.1186/cc11455, PMID 23394215

13. Rushdi MI, Abdel-Rahman IA, Saber H, Attia EZ, Abdelraheem WM, Madkour HA. Pharmacological and natural products diversity of the brown algae genus *Sargassum*. RSC Adv. 2020;10(42):24951-72. doi: 10.1039/d0ra03576a, PMID 35517468
14. Hima RV, Harikrishnan S, Parivallal M, Rahman MS, Basha SM, Sreedhar K. Analysis of the chemical, nutrient and physicochemical properties of brown macroalgae, *Sargassum ilicifolium* collected from Mandapam coast, Rameshwaram. Biochem Cell Arch. 2023 Sep 15;23(2):1029-36. doi: 10.51470/bca.2023.23.2.1029
15. Torres-Narváez A, Olvera-Ramírez AM, Castaño-Sánchez K, Chávez-Servín JL, Reis De Souza TC, McEwan NR. Therapeutic and nutraceutical potential of *Sargassum* species: A narrative review. Mar Drugs. 2025;23(9):343. doi: 10.3390/md23090343, PMID 41003312
16. Saraswati, Giriwono PE, Iskandriati D, Andarwulan N. Screening of *in-vitro* anti-inflammatory and antioxidant activity of *Sargassum ilicifolium* crude lipid extracts from different coastal areas in Indonesia. Mar Drugs. 2021 Apr 28;19(5):252. doi: 10.3390/md19050252, PMID 33925071
17. Purohit P, Kataria MK. Phytochemicals screening, antioxidant and antimicrobial activity of *Carica* papaya leaf extracts. Int J Curr Pharm Res. 2024;16(3):95-8. doi: 10.22159/ijcpr.2024v16i3.4087
18. Avalappa HE, Padiyappa SD, Pathappa NI, Bettadatunga PT, Pramod SN. Legume Indian bean (*Phaseolus vulgaris*) partially purified anti-nutritional protein factor exhibit anti-oxidant, immunomodulatory and anti-cancer properties. Int J Pharm Pharm Sci. 2023;15(2):8-17. doi: 10.22159/ijpps.2023v15i2.46831
19. Saeed NA, Rasool AM, Zeebaree AY. Anti-cancer possibility of zingier officiale nanoparticles: Mechanisms and therapeutic understanding. Int J Appl Pharm. 2025;17(6):417-22. doi: 10.22159/ijap.2025v17i6.55836
20. Xu S, Gao Y, Zhang Q, Wei S, Chen Z, Dai X. SIRT1/3 activation by resveratrol attenuates acute kidney injury in a septic rat model. Oxid Med Cell Long. 2016;2016:7296092. doi: 10.1155/2016/7296092
21. Vishwanadham Rao V, Narayanappa Shanti K, Manjegowda DS. Molecular docking and graphical trajectory analysis of *Cinnamomum zeylanicum* compounds for targeting human maltase-glucoamylase in diabetes management. Int J Appl Pharm. 2025 Nov 7;17(6):367-80.
22. Vijayabaskaran M, Sivakumar P, Sambathkuamr R, Perumal P, Sivakumar T, Jayakar B. Anti-inflammatory and toxicity evaluation of ethyl-ethyl-propyl-valerate (EEPV) in albino rats: Application of OECD guidelines for testing of chemicals (Test No. 423). Int J Chem Res. 2011;2(4):4-7.
23. Rehman MU, Tahir M, Ali F, Qamar W, Lateef A, Khan R. Cyclophosphamide-induced nephrotoxicity, genotoxicity, and damage in kidney genomic DNA of Swiss albino mice: The protective effect of ellagic acid. Mol Cell Biochem. 2012 Jun;365(1-2):119-27. doi: 10.1007/s11010-012-1250-x, PMID 22286819
24. Ajiboye BO, Famusiwa CD, Nifemi DM, Ayodele BM, Akinlolu OS, Fatoki TH. Nephroprotective effect of *Hibiscus sabdariffa* leaf flavonoid extracts via KIM-1 and TGF-1β signaling pathways in streptozotocin-induced rats. ACS Omega. 2024 Apr 19;9(17): 19334-44. doi: 10.1021/acsomega.4c00254, PMID 38708257
25. Khalil AM, Kasem NR, Ali AS, Salman MM. Brown seaweed *Sargassum cinereum* extract ameliorates the hepato and nephrotoxicity induced by cyclophosphamide in male albino rats: Hematological Biochemical and histobiochemical examinations. Saudi J Pathol Microbiol. 2020 Feb 29;5(2):86-94. doi: 10.36348/sjpm.2020.v05i02.009
26. Yang J, Kwon YS, Kim MJ. Isolation and characterization of bioactive compounds from *Lepisorus thunbergianus* (Kaulf.). Arab J Chem. 2015 May 01;8(3):407-13. doi: 10.1016/j.arabjc.2014.11.056
27. Abdel-Daim MM, Abushouk AI, Abdeen A, Halawa SM, Khalifa HA. Antioxidant and nephroprotective effects of polyphenol-rich plant extracts in drug-induced kidney injury. Biomed Pharmacother. 2018;97:1681-9.
28. Wang J, Guo HM. Astragaloside IV ameliorates high glucose-induced HK-2 cell apoptosis and oxidative stress by regulating the Nrf2/ARE signaling pathway. Exp Ther Med. 2019;17(6):4409-16. doi: 10.3892/etm.2019.7495, PMID 31086575
29. Bao L, Li J, Zha D, Zhang L, Gao P, Yao T. Chlorogenic acid prevents diabetic nephropathy by inhibiting oxidative stress and inflammation through modulation of the Nrf2/HO-1 and NF-κB pathways. Int Immunopharmacol. 2018;54:245-53. doi: 10.1016/j.intimp.2017.11.021, PMID 29161661
30. Zhang Y, Li Y, Zhang J, Wang L, Chen X, Liu Q. Chlorogenic acid prevents diabetic nephropathy by inhibiting oxidative stress and inflammation through modulation of the Nrf2/HO-1 and NF-κB pathways. J Diabetes Res. 2017;2017:9645238. doi: 10.1155/2017/9645238